www.czasopisma.pan.pl PAN POLSKA AKADEMIA NAUK www.journals.pan.pl

ARCHIVES OF ACOUSTICS Online First September 26, 2024 doi: 10.24425/aoa.2024.148810

Research Paper

Sound Insulation of an Acoustic Barrier with Layered Structures of Sonic Crystals – Comparative Studies of Physical and Theoretical Models

Jan RADOSZ

Central Institute for Labour Protection – National Research Institute
Warsaw, Poland; e-mail: jarad@ciop.pl

(*received March 2, 2022; accepted June 11, 2024; published online September 26, 2024*)

Recent years have seen a growing interest in the potential for the use of sonic crystals as noise barriers. The frequencies with the highest attenuation can be determined by assuming that an integer number of half wavelengths fits the distance between the scatterers. However, this approach limits the usefulness of sonic crystals as a viable noise barrier technology, as it necessitates a significant increase in the overall crystal size to cover a broader frequency range for noise reduction. Based on developed theoretical models, geometrical assumptions were made for the physical models of the acoustic barrier in terms of the materials used and the dimensions of structural elements. Three physical models were developed to verify the design intent. The method involved measuring the transmission loss (TL) and insertion loss (IL) of the sonic crystal structure and comparing these results with theoretical models. The aim of this work was to perform free-field measurements on a real-sized sample in order to verify the strengths and weaknesses of applying layered structures of sonic crystals based on calculations and measurements. The results of the conducted measurements showed satisfactory noise reduction by the developed physical models for key components of the analysed spectrum. It was also demonstrated that layered structures of sonic crystals can achieve greater noise reduction (up to 3.5 dB) and a wider frequency range of attenuation (up to the range of 2000 Hz–5000 Hz) compared to single-layer structures.

Keywords: noise; barrier; sonic crystal; diffuser.

1. Introduction

Sonic crystals have received significant attention from the acoustical community over the past decade because of their unique acoustic properties. The ability of sonic crystals to function as stop-band filters in the audible frequency range, i.e., to attenuate waves within frequency bands known as band gaps, is the most attractive and extensively studied property of such materials. Further advantages of sonic crystal barrier in comparison to traditional sound barriers, include their ability to allow light to pass through and, uniquely, their non-obstruction of the free flow of air. The existence of band gaps in sonic crystals was demonstrated in early works (MARTINEZ-SALA *et al.*, 1995; RUBIO *et al.*, 1999; SÁNCHEZ-PÉREZ *et al.*, 1998). However, barriers made from these "conventional" sonic crystals suffer from the major disadvantage of providing attenuation only within a relatively narrow frequency band and are therefore unsuitable as barriers for broad-band noise attenuation. To enhance the sound insulation properties of sonic crystals, researchers have recently focused on systems in which both Bragg scattering and local resonant phenomena are present (ELFORD *et al.*, 2011; FUSTER-GARCIA *et al.*, 2007; GOFFAUX, SÁNCHEZ-DEHESA, 2003; HIRSEKORN *et al.*, 2004; HO *et al.*, 2003; LIU *et al.*, 2000; ROMERO-GARCIA *et al.*, 2013; HU *et al.*, 2005; CASTIÑEIRA-IBAÑEZ *et al.*, 2012). These investigations showed that periodic arrays of scatterers composed of a small number of elements are capable of achieving sound attenuation values large enough to compete with other acoustic barriers.

To measure the effective screening effect of a barrier, MORANDI *et al.* (2016) proposed using transient sound signals and a suitable windowing technique, which is now standardised in EN 1793-6 (CEN, 2012). The paper aims to conduct laboratory testing of scat-

terers to experimentally determine their acoustic performance. According to two studies (Morandi *et al.*, 2015; 2016), the availability of standardised values allows a direct comparison of the sound insulation and reflection properties of the sonic crystal noise barriers related to other classical. However, the results of measurements presented in the paper indicate that the number of measurement points according to EN 1793-6 (CEN, 2012) may not be sufficient.

In previous research (Radosz, 2019), the author explored the potential of sonic crystals as noise barriers, highlighting their ability to create band gaps that attenuate sound waves. The study focused on a multiple-resonance band gap system to enhance sound attenuation properties, using six concentric *C*-shaped resonators. However, the research identified limitations in the frequency range of attenuation, primarily due to the specific lattice parameters and packing fraction of the sonic crystals used. Further research is needed to evaluate layered structures of sonic crystals in terms of increasing sound insulation with a possible synergy effect of layers.

2. Materials and methods

The study is organised as follows. According to data obtained from measurements of a compressor unit (Fig. 1), single unit cells are studied by means of finite element (FE) Bloch-type analyses in order to investigate the band structure of the unit cells to identify those capable of generating band gaps.

2.1. Analyses of band structures

Numerical analyses were performed to design a basic sonic crystal single-layer structure exhibiting a complete band gap within the frequency range in which the compressor noise spectrum shows a prominent peak (see Fig. 1). The lattice constant is set in accordance to Bragg scattering theory, looking for a band gap at approximately 2900 Hz and 4500 Hz corresponding to the FFT spectrum of the compressor unit (see Fig. 1). The resulting lattice constants for layers are 38 mm (A-1) and 60 mm (A-2), given $c_{\text{air}} = 343$ m/s, the speed of sound in air at 20 °C. PVC pipes with radii of 28 mm (A-1) and 44 mm (A-2) were considered as inclusion placed at the centre of the unit cell. The properties of the materials used in the calculations are listed in Table 1.

Table 1. Properties of material and medium used in the FE analyses.

Material/ medium	Density ρ [kg/m^{-3}]	Longitudinal wave c_L [m·s^{-1}]	Shear wave speed c_S [m·s^{-1}]
Air	1.25	343	–
PVC	1400	2142	874

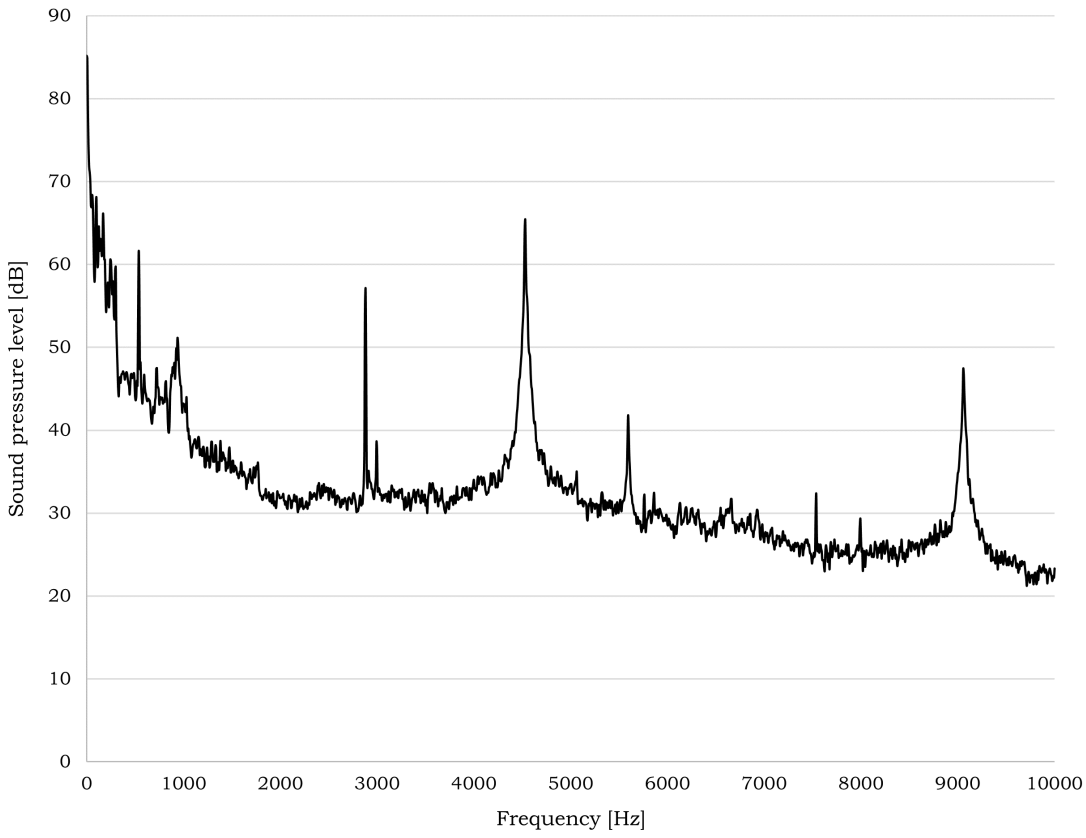

Fig. 1. Fast Fourier transform (FFT) spectrum at the measuring point at the inlets of an industrial compressor unit.

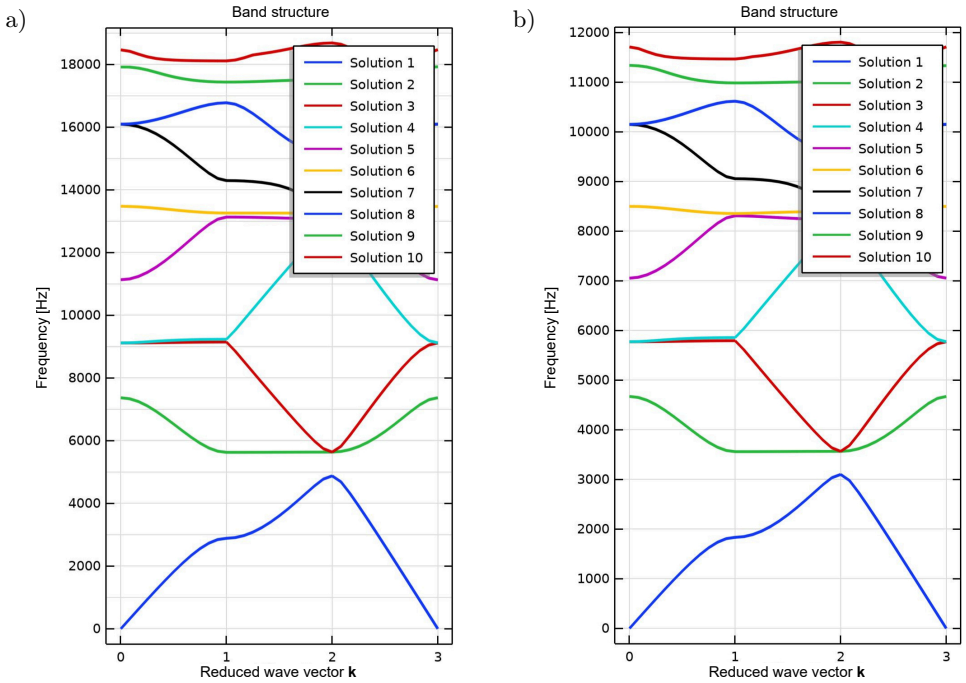

Fig. 2. Band structures for air-PVC pipe unit cell in the first irreducible Brillouin zone (for ten eigenfrequencies solutions): a) model A-1; b) model A-2.

The band structure was computed along the three high-symmetry directions of the first irreducible Brillouin zone ΓX, XM, and $M\Gamma$ using the plane wave expansion (PWE) method with the use of MATLAB software. Figure 2 presents the band structures in terms of the reduced wave vector $\mathbf{k} = \left[\frac{k_x a}{\pi}; \frac{k_y a}{\pi}\right]$, where $\mathbf{k}_x$ and $\mathbf{k}_y$ are the wave vectors in the x and y directions, respectively.

2.2. Design assumptions of physical models of the acoustic barrier

It was assumed that the three physical models proposed, based on selected theoretical models, are designed using commonly available materials with standardised dimensions (pipes, profiles, etc.). The physical model is made from PVC pipes (diffusers) with a density of $\rho = 1400$ kg/m^{-3}. The foundations of the physical models are made from MDF boards. The dimensions of the physical models are shown in Figs. 3–5.

2.3. Measurement method

The measurements of transmission loss (TL) were carried out using a laboratory stand, the scheme of which is shown in Fig. 6. According to the adopted test method, the stand was located in an anechoic chamber in order to ensure acoustic conditions similar to those

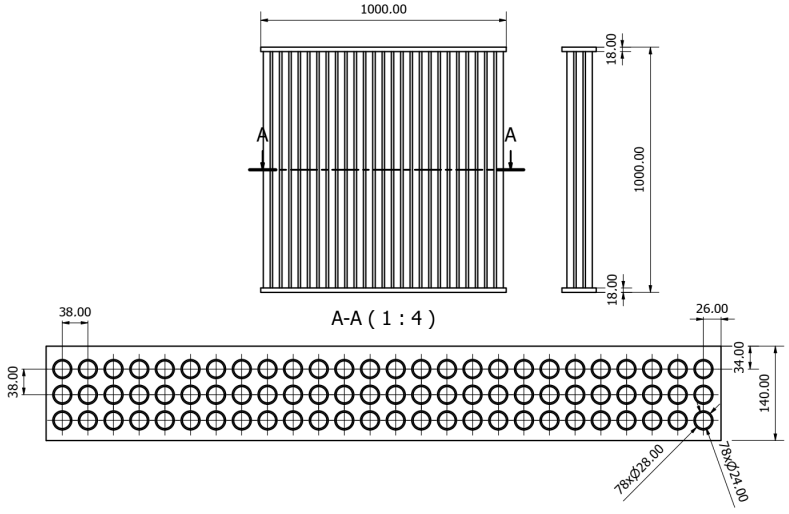

Fig. 3. Dimensions of the A-1 physical model of the acoustic barrier.

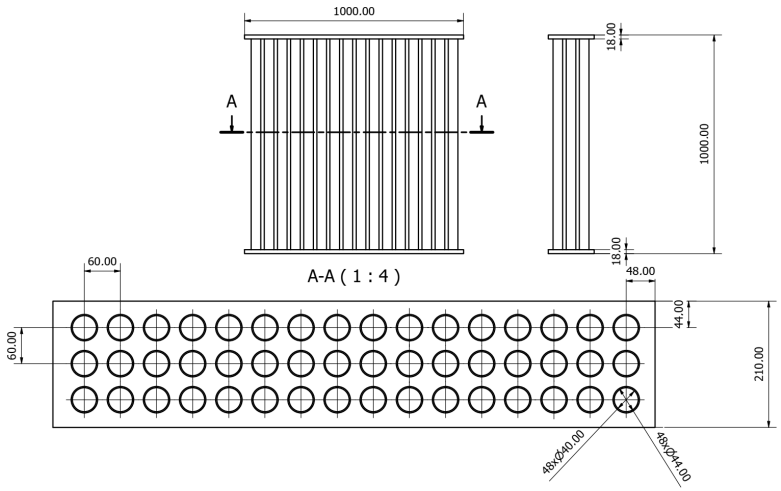

Fig. 4. Dimensions of the A-2 physical model of the acoustic barrier.

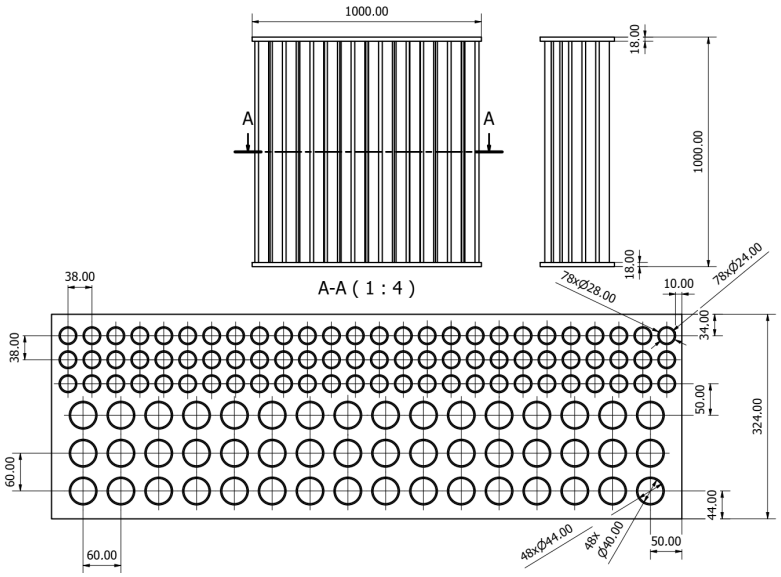

Fig. 5. Dimensions of the A-3 physical model of the acoustic barrier.

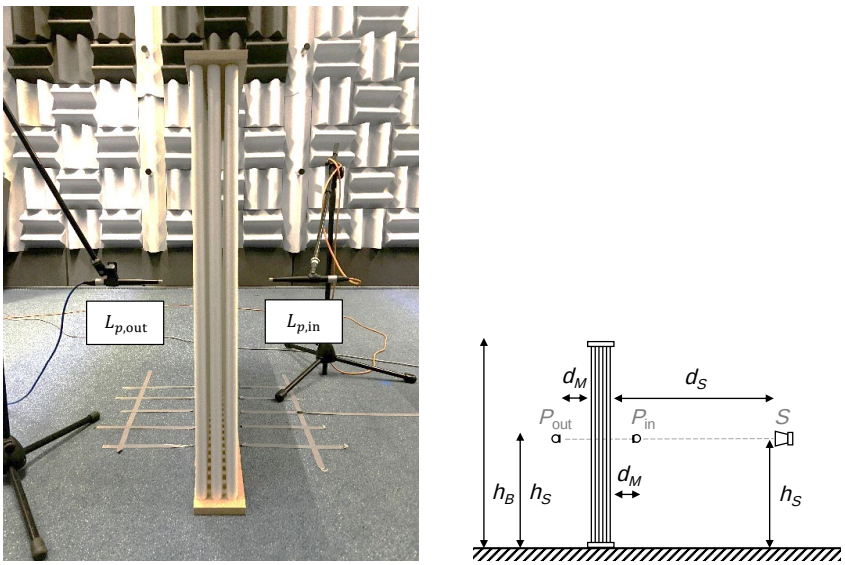

Fig. 6. Scheme of the laboratory stand for measuring TL: S – sound source; P_{in}, P_{out} – measurements points; h_S = 0.5 m; h_B = 1 m; d_M = 0.1 m; d_S = 1 m.

of a free field, which were used in the theoretical model tests.

The tested physical models of the acoustic barrier were situated on the floor structure. The positioning of the sound source and microphones in relation to the physical model corresponded to the setup adopted in the computational model.

The sound source (Bose S1 PRO) was placed at a distance of 100 cm from the model surface, with its main radiation axis perpendicular to the surface and passing through the centre of the model.

Microphones (DPA 4007) were placed successively at five points, spaced 10 cm apart, on the horizontal centreline of the module, at a distance of 10 cm from the model's surface.

The values of sound pressure levels for 1/3 octave bands were calculated from the impulse responses obtained with the use of maximum length sequence (MLS) signal (DIRAC software). Then, the values of sound TL were determined according to the following equation:

$$\mathrm{TL} = \overline{L_{p,\mathrm{in}}} - \overline{L_{p,\mathrm{out}}} \ [\mathrm{dB}],$$

where $\overline{L_{p,\mathrm{in}}}$ is the mean sound pressure level from five measurement points in front of the barrier, and $\overline{L_{p,\mathrm{out}}}$ is the mean sound pressure level from five measurement points behind the barrier.

The values of insertion loss (IL) were determined based on the measured values of the sound pressure levels in the space behind the screen $\overline{L_{p,1}}$ (mean value from five measurement points) and in the space without the acoustic barrier $\overline{L_{p,2}}$ (mean value from five measurement points), assuming the same distances as specified in the EN 1793-6 (CEN, 2012) (Fig. 7).

Figure 8 shows the highest values of the repeatability standard deviation for three measurements performed at each measurement point using the impulse response with the MLS signal. These values did not exceed 0.022 dB, which indicates a high repeatability of the measurement method used.

2.4. Measurement results

Figures 9–11 present a comparison of TL (calculated as the average from five measurement points) between theoretical models and physical models of the acoustic barrier. The measurement results showed that the occurrence of the band gap was consistent with the results of theoretical calculations for the key spectrum bands resulting from Bragg's law.

For the case of the A-1 physical model (measurements), the highest attenuation was obtained in the third octave band with a centre frequency of 4000 Hz. The measured TL was 19.7 dB, which differs by 0.7 dB

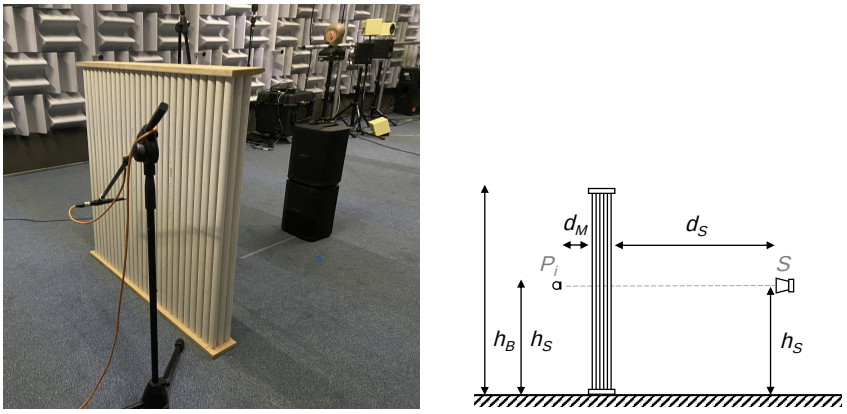

Fig. 7. Scheme of the laboratory stand for measuring IL: S – sound source; P_i – measurements points; $h_S = 0.5$ m; $h_B = 1$ m; $d_M = 0.25$ m; $d_S = 1$ m.

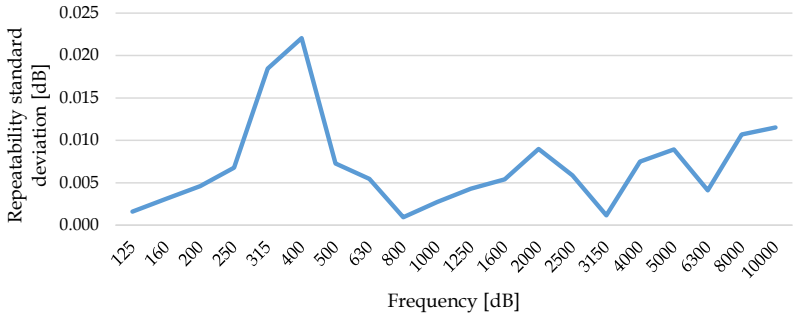

Fig. 8. Repeatability standard deviation of the measurements using the impulse response with the MLS signal (highest value from five measurement points).

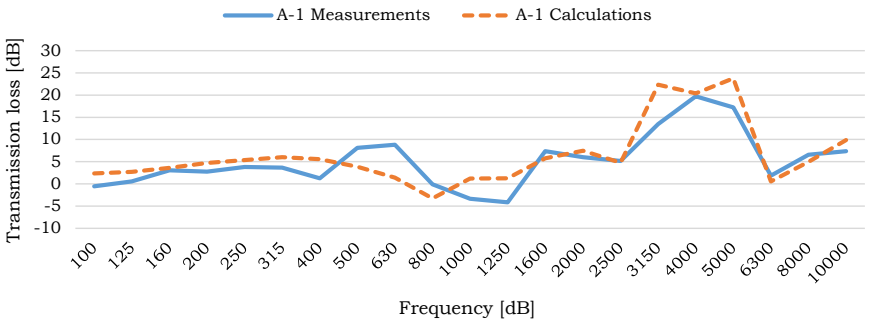

Fig. 9. Comparison of TL results for A-1 model.

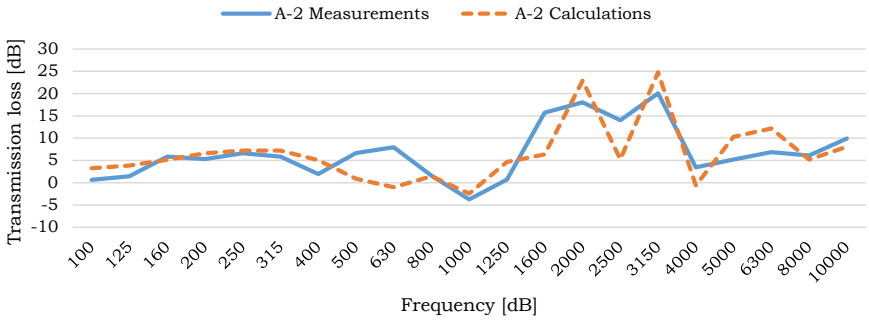

Fig. 10. Comparison of TL results for A-2 model.

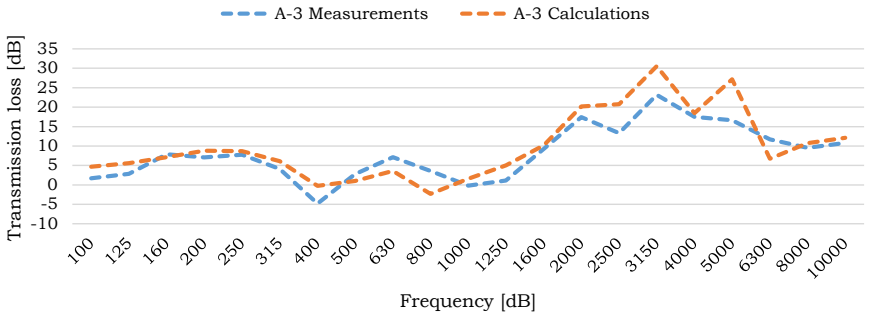

Fig. 11. Comparison of TL results for A-3 model.

from the theoretical model (calculations) for that band (Fig. 9).

For the A-2 physical model, the highest attenuation was achieved in the 1/3 octave bands with centre frequencies of 2000 Hz and 3150 Hz. The measured TLs were 18.0 dB and 20.1 dB, respectively (Fig. 10). The differences from the theoretical model for these bands were 4.8 dB and 4.7 dB.

In the case of the A-3 physical model, the highest attenuation was achieved in the 1/3 octave bands with centre frequencies ranging from 2000 Hz to 5000 Hz. The measured TLs varied from 13.3 dB to 23.2 dB (Fig. 11). The differences with the theoretical model in this range were between 1.0 dB and 10.6 dB.

Figures 12–14 present a comparison of IL (calculated as the average from five measurement points) between theoretical models and physical models of the acoustic barrier. The results of the measurements showed that the occurrence of the band gap was consistent with the results of theoretical calculations for the key spectrum bands predicted by Bragg's law.

In the case of the A-1 model, the highest attenuation was observed in the 1/3 octave bands with centre frequencies ranging from 4000 Hz to 5000 Hz. The measured ILs were 14.7 dB and 15.5 dB, respectively (Fig. 12). The differences from the theoretical model for the 1/3 octave bands with centre frequencies of 4000 Hz and 5000 Hz were 4.1 dB and 0.6 dB, respectively.

In the case of the A-2 physical model, the highest attenuation was achieved in the 1/3 octave bands with centre frequencies ranging from 2000 Hz to 3150 Hz. The measured ILs were from 13.0 dB to 16.4 dB (Fig. 13). The differences from the theoretical model in this range were from 2.3 dB to 3.4 dB.

In the case of the A-3 physical model, the highest attenuation was achieved in the 1/3 octave bands with centre frequencies ranging from 2000 Hz to 5000 Hz.

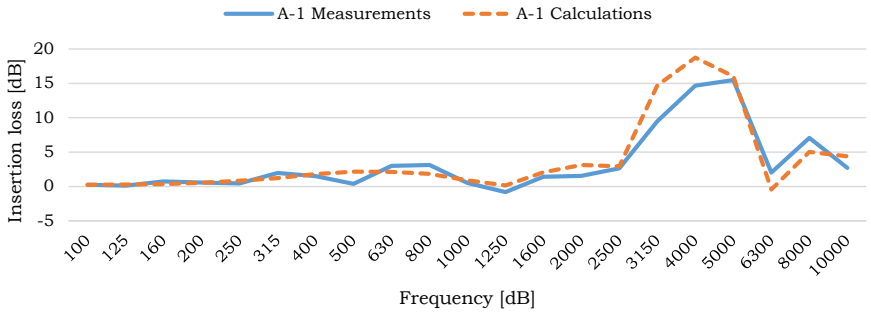

Fig. 12. Comparison of IL results for A-1 model.

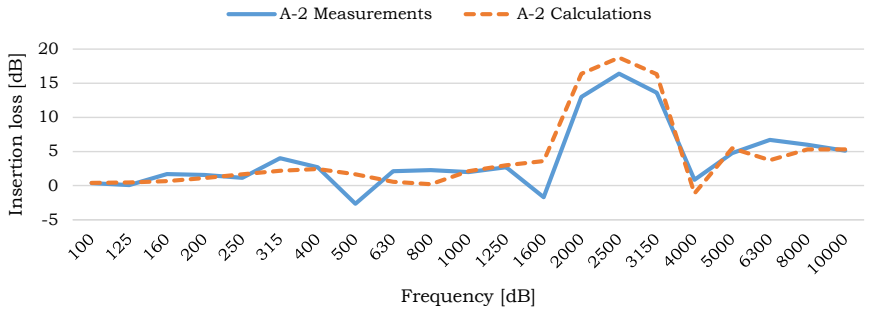

Fig. 13. Comparison of IL results for A-2 model.

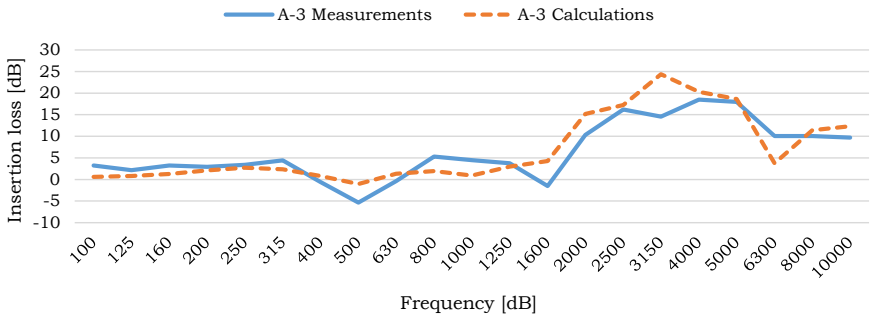

Fig. 14. Comparison of IL results for A-3 model.

The measured ILs were ranging from 10.3 dB to 18.5 dB (Fig. 14). The differences from the theoretical model in this range ranged from 0.7 dB to 9.8 dB.

Figure 15 presents a comparison of the measurement results for TL and IL across the three physical models of the acoustic barrier (A-1–A-3). In both cases, it was shown that the layered physical model (A-3) provides greater noise attenuation and a wider frequency range of attenuation compared to the single-layer structures (A-1 and A-2).

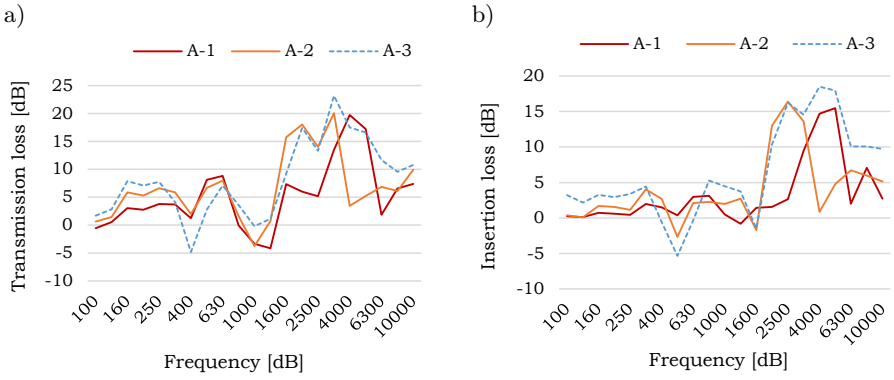

Fig. 15. Comparison of TL (a) and IL (b) measurement results for three physical models.

3. Conclusions

Compared to traditional partitions, barriers composed of sonic crystal structures do not exhibit continuous attenuation characteristics. The developed proposals of physical models, including layered structures, provide great opportunities for noise reduction in frequency bands where industrial noise sources emit substantial acoustic energy and significantly increase the frequency range of sound attenuation.

Three physical models were developed based on theoretical models. A laboratory test stand was prepared in a test room with conditions similar to a free field. The effectiveness of noise attenuation for sonic crystal structures was assessed using impulse response measurements for samples measuring 1 m × 1 m.

The results of the conducted measurements showed that the noise attenuation provided by the developed physical models was satisfactory for the key components of the analysed spectrum. It was also demonstrated that the layered structure allows to increase the noise attenuation (up to 3.5 dB) and increase the frequency range of attenuation (up to the range of 2000 Hz–5000 Hz) compared to single-layer structures. The measured of TL for the multilayer model was 23.3 dB, while the IL was 18.5 dB. The method used produced repeatable measurement results, with a standard deviation of repeatability not exceeding 0.02 dB.

The design assumptions were verified by comparing the measurement results of the physical models with those from theoretical models. The comparison of the results showed consistency in the occurrence of band gaps for key spectral bands predicted by Bragg's law, for both the TL and IL. Despite this agreement and the satisfactory effectiveness of noise suppression, differences were observed between the values in TL and IL between the physical and theoretical models. These differences result from the fact that theoretical models are 2D models and do not take into account the finite height of the barrier and the influence of the ground. The study results help estimate the influence of factors such as sound reflections or diffraction, which are not considered in 2D theoretical models.

Acknowledgments

This paper is based on research conducted as part of the fifth stage of the National Programme "Improvement of Safety and Working Conditions" partially supported from 2020 to 2022 by the Polish National Centre for Research and Development (project no.III.PB.01 titled "Development of an Industrial Acoustic Barrier for Attenuation of Narrowband Noise Components Using Layered Structures of Phonic Crystals").

The Central Institute for Labour Protection – National Research Institute in Poland is the Programme's main coordinator.

References

1. Castiñeira-Ibáñez S., Rubio C., Romero-García V., Sánchez-Pérez J.V., García-Raffi L.M. (2012), Design, manufacture and characterization of an acoustic barrier made of multi-phenomena cylindrical scatterers arranged in a fractal-based geometry, *Archives of Acoustics*, **37**(4): 455–462, doi: 10.2478/v10168-012-0057-9.

2. CEN (2012), *Road traffic noise reducing devices – Test method for determining the acoustic performance – Part 6: Intrinsic characteristics – In situ values of airborne sound insulation under direct sound field conditions*, EN 1793-6:2012.

3. Elford D.P., Chalmers L., Kusmartsev F.V., Swallowe G.M. (2011), Matryoshka locally resonant sonic crystal, *The Journal of the Acoustical Society of America*, **130**(5): 2746–2755, doi: 10.1121/1.3643818.

4. Fuster-Garcia E., Romero-García V., Sánchez-Pérez J.V., García-Raffi L.M. (2007), Targeted band gap creation using mixed sonic crystal arrays including resonators and rigid scatterers, *Applied Physics Letters*, **90**(24): 244104, doi: 10.1063/1.2748853.

5. Goffaux C., Sánchez-Dehesa J. (2003), Two-dimensional phononic crystals studied using a variational method: Application to lattices of locally resonant materials, *Physical Review B*, **67**(14): 144301, doi: 10.1103/PhysRevB.67.144301.

6. Hirsekorn M., Delsanto P.P., Batra N.K., Matic P. (2004), Modelling and simulation of acoustic wave propagation in locally resonant sonic materials, *Ultrasonics*, **42**(1–9): 231–235, doi: 10.1016/j.ultras.2004.01.014.

7. Ho K.M., Chun K.C., Yang Z., Zhang X.X., Sheng P. (2003), Broadband locally resonant sonic shields, *Applied Physics Letters*, **83**(26): 5566–5568, doi: 10.1063/1.1637152.

8. Hu X., Chan C.T., Zi J. (2005), Two-dimensional sonic crystals with Helmholtz resonators, *Physical Review E*, **71**(5): 055601(R), doi: 10.1103/PhysRevE.71.055601.

9. Liu Z. *et al.* (2000), Locally resonant sonic materials, *Science*, **289**(5485): 1734–1736, doi: 10.1126/science.289.5485.1734.

10. Martínez-Sala R., Sancho J., Sánchez J.V., Gómez V., Llinares J., Meseguer F. (1995), Sound attenuation by sculpture, *Nature*, **378**(6554): 241, doi: 10.1038/378241a0.

11. Morandi F., Miniaci M., Guidorzi P., Marzani A., Garai M. (2015), Acoustic measurements on a sonic crystals barrier, *Energy Procedia*, **78**: 134–139, doi: 10.1016/j.egypro.2015.11.128.

12. Morandi F., Miniaci M., Marzani A., Barbaresi L., Garai M. (2016), Standardised acoustic char-

acterisation of sonic crystals noise barriers: Sound insulation and reflection properties, *Applied Acoustics*, **114**: 294–306, doi: 10.1016/j.apacoust.2016.07.028.

13. Radosz J. (2019), Acoustic performance of noise barrier based on sonic crystals with resonant elements, *Applied Acoustics*, **155**: 492–499, doi: 10.1016/j.apacoust.2019.06.003.

14. Romero-García V., Krynkin A., Garcia-Raffi L.M., Umnova O., Sánchez-Pérez J.V. (2013), Multi-resonant scatterers in sonic crystals: Locally multi-resonant acoustic metamaterial, *Journal of Sound and Vibration*, **332**(1): 184–198, doi: 10.1016/j.jsv.2012.08.003.

15. Rubio C. *et al.* (1999), Existence of full gaps and deaf bands in two-dimensional sonic crystals, *Journal of Lightwave Technology*, **17**(11): 2202–2207, doi: 10.1109/50.803012.

16. Sánchez-Pérez J.V. *et al.* (1998), Sound attenuation by a two-dimensional array of rigid cylinders, *Physical Review Letters*, **80**: 5325, doi: 10.1103/PhysRevLett.80.5325.